Title

Neutral-neutral Reactions in the Interstellas Medium. I.Formation of Carbon hydride radicals via reaction of carbon atoms with unsaturated hydrocarbons

Journal

Astrophysical journal, 477

Author

Kaiser, R.I.

Publication Date

1996-07-01

LBNL-38943
UC-401
Preprint

ERNEST ORLANDO LAWRENCE
BERKELEY NATIONAL LABORATORY

Neutral-Neutral Reactions in the Interstellar Medium I: Formation of Carbon Hydride Radicals via Reaction of Carbon Atoms with Unsaturated Hydrocarbons

R.I. Kaiser, D. Stranges, Y.T. Lee, and A.G. Suits
Chemical Sciences Division

July 1996
Submitted to
The Astrophysical Journal

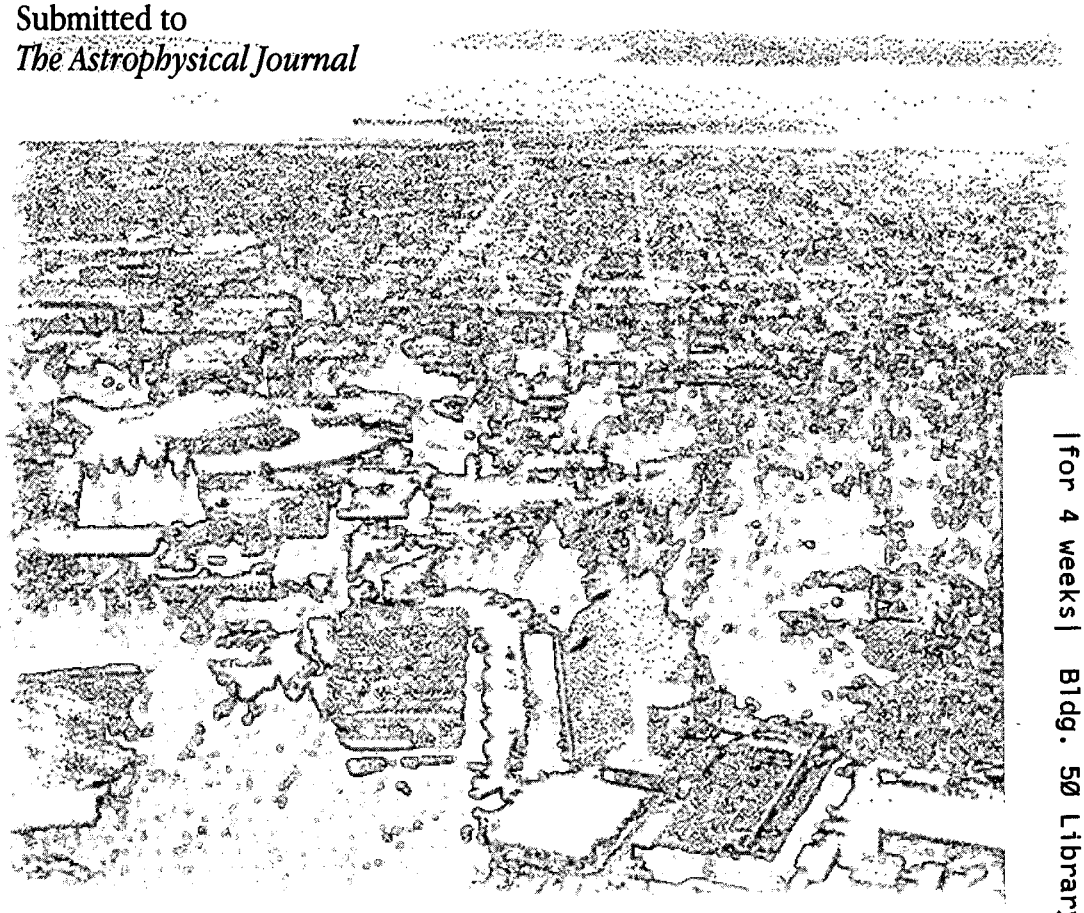

DISCLAIMER

LBNL-38943
UC-401

Neutral-Neutral Reactions in the Interstellar Medium I: Formation of Carbon Hydride Radicals via Reaction of Carbon Atoms with Unsaturated Hydrocarbons

R.I. Kaiser,[1*] D. Stranges,[1**] Y.T. Lee,[2] and A.G. Suits[1†]

[1]Department of Chemistry
University of California
and
Chemical Sciences Division
Ernest Orlando Lawrence Berkeley National Laboratory
University of California
Berkeley, California 94720

[2]Academia Sinica
Nankang, Taipei 11529, Taiwan

July 1996

*E-mail Address: kaiser@leea.cchem.berkeley.edu
**Present Address: Dipartimento Chimica, Universita La Sapienza, Piazzale A. Moro 5, 00185 Rome, Italy. E-mail address: dstranges@axrma.uniroma1.it
†E-mail Address: agsuits@lbl.gov

This work was supported by the Director, Office of Energy Research, Office of Basic Energy Sciences, Chemical Sciences Division, of the U.S. Department of Energy under Contract No. DE-AC03-76SF00098.

ABSTRACT

The reactions of atomic carbon in its ^3P_j electronic ground state with acetylene, C_2H_2 (1), methylacetylene, CH_3CCH (2), ethylene, C_2H_4 (3), and propylene, C_3H_6 (4), were investigated at relative collision energies between 8.8 and 45 $kJmol^{-1}$ in crossed beam experiments to elucidate the reaction products and chemical dynamics of atom-neutral encounters relevant to the formation of carbon bearing molecules in the interstellar medium (ISM). Reactive scattering signal was found at m/e = 37, 51, 39, and 53, i.e. C_3H (1), as well as the hitherto unobserved interstellar radicals C_4H_3 (2), C_3H_3 (3), and C_4H_5 (4). All reactions proceed on the triplet surface via addition of the carbon atom to form propendi-ylidene and cyclopropenylidene, C_3H_2 (1), 1-methylpropendiylidene, C_4H_4 (2), cyclopropylidene, C_3H_4 (3), as well as methylcyclopropylidene, C_4H_6 (4). The initial collision complexes undergo hydrogen migration (1/2) or ring opening (3/4) and decompose via C-H-bond rupture to l/c-C_3H (1), n-C_4H_3 (2), propargyl (3), and methylpropargyl (4). The explicit identification of the carbon-hydrogen exchange channel under single collision conditions identifies this class of reaction as a potential pathway to carbon-bearing species in the ISM. Our findings strongly demand the incorporation of distinct structural isomers in prospective chemical models of interstellar clouds, hot cores, and circumstellar envelopes around carbon stars.

Subject headings: ISM: molecules - methods: laboratory - molecular processes

1. INTRODUCTION

Carbon chains and cyclic molecules are common constituents of interstellar clouds, hot cores, and circumstellar envelopes of carbon stars. Hitherto, the homologous series HC_n (n = 1 - 6), C_n (n = 1, 2, 3, 5), H-$(C{\equiv}C)_n$-CN (n = 0 - 4), $(C{\equiv}C)_n$-CN (n = 0, 1), CH_3-$(C{\equiv}C)_n$-CN (n = 0 - 2), H_2C_n (n = 3, 4), C_nO (n = 1 - 3), C_nS (n = 1, 2, 3, 5), and C_nSi (n = 4) as well as the cyclic compounds c-SiC_2, c-C_3H_2, and c-C_3H have been assigned (Scheffler & Elsässer 1988; Irvine 1992; Cowley 1995). Among them, linear C_3H, l-C_3H (propynylidyne), was detected by Thaddeus et al. (1985) via microwave spectroscopy toward the dark Taurus Molecular Cloud 1 (TMC-1) and the carbon star IRC +10216. Two years later, Yamamoto et al. (1987) identified rotational transitions of the cyclic isomer, c-C_3H (cyclopropynylidyne), in TMC-1 prior to laboratory synthesis (Yamamoto & Saito 1990). Although thermally unstable and extremely reactive in terrestrial laboratories, l/c-C_3H hold high fractional abundances of $1.0{\pm}0.7{*}10^{-9}$ in TMC-1 (Thaddeus, Vrtilek, & Gottlieb 1985), about one order of magnitude less than the ubiquitous cyclopropenylidene, c-C_3H_2.

Despite their large interstellar number densities, synthetic routes have not yet been fully resolved. Since the average kinetic energy of interstellar species is

confined to typically 0.8 $kJmol^{-1}$ (diffuse clouds) and 0.08 $kJmol^{-1}$ (dark, molecular clouds), gas phase reactions under thermodynamical equilibrium conditions must have little or no barriers and involve only two body collisions. Ternary encounters occur only once in a few 10^9 years and can be neglected considering mean interstellar cloud lifetimes of 10^6 years. Therefore, chains of radiative association, dissociative recombination, as well as exothermic ion-molecule reactions have dominated generic chemical models for over more than two decades (Herbst & Klemperer 1973; Herbst & Delos 1976; Williams 1979; Herbst, Adams, & Smith 1984; Winnewisser & Herbst 1987; Sternberg & Dalgarno 1995; Gerlich & Horning 1992; Smith 1992). The inclusion of exothermic neutral-neutral encounters into chemical models, e.g. of the circumstellar envelope surrounding the carbon star IRC+10216 and the dark cloud TMC-1, occurred only gradually (Graff 1989; Millar, Leung, & Herbst 1990; Herbst & Leung 1990; Clary, Stoecklin, & Wickham 1993; Herbst et al. 1994; Millar & Herbst 1994; Bettens & Herbst 1995; Liao & Herbst 1995; Bettens, Lee, & Herbst 1995), predominantly because entrance barriers were assumed to hinder this reaction class.

Recently, Husain and coworkers investigated rate constants of $C(^3P_j)$ with unsaturated hydrocarbons monitoring the decay kinetics of $C(^3P_j)$ at room temperature (Haider & Husain 1993; Husain 1993; Clary et al. 1994). These bulk experiments indicated reactions proceed barrier-less and rapidly ($k = 10^{-10} - 10^{-9}$

cm^3s^{-1}) within orbiting limits (Levine & Bernstein 1987). Likewise, kinetic studies of neutral-neutral reactions involving, e.g., OH, CN, and CH radicals at ultralow temperatures reveal rate constants about $1\text{-}6*10^{-10}$ cm^3s^{-1} with maxima between 50 - 70 K, and only a slight decrease as the temperature falls to 13 K (Sims et al. 1992; Sims et al. 1993; Sims et al. 1994a; Sims et al. 1994b; Canosa et al. 1996). Despite valuable kinetic data, reaction products cannot be probed experimentally, and the outcome of neutral-neutral reactions incorporated into interstellar chemical models is predominantly postulated based on spin conservation as well as thermochemistry without investigating distinct structural isomers. This shortcoming clearly demonstrates the urgency of systematic laboratory examinations to elucidate detailed chemical dynamics as well as the reaction products of neutral-neutral encounters relevant to interstellar chemistry.

Here, we investigate the following reactions of atomic carbon in its electronic ground state, $C(^3P_j)$, as a potential source of interstellar carbon hydride radicals (Fig. 1):

(1) $C(^3P_j) + C_2H_2 \rightarrow C_3H + H$

(2) $C(^3P_j) + CH_3CCH \rightarrow C_4H_3 + H$

(3) $C(^3P_j) + C_2H_4 \rightarrow C_3H_3 + H$

(4) $C(^3P_j) + C_3H_6 \rightarrow C_4H_5 + H.$

Owing to the high reactivity of prospective open shell products, experiments must be performed under single collision conditions to identify the primary reaction products without collisional stabilization or successive reaction of the initially formed complex. Further, hydrocarbon radicals with often unknown spectroscopic properties have to be probed. The requirements are achieved in our studies using the crossed molecular beam technique as described extensively in Lee et al. 1969 and Lee 1988. The reaction channels and selected center-of-mass flux contour plots are presented in § 3 together with results of translational energy distributions and angular distributions in the center-of-mass reference frame. Chemical dynamics and potential energy surfaces (PES) are outlined in § 4. Finally, astrophysical implications are discussed in § 5.

2. EXPERIMENTAL PROCEDURE AND DATA PROCESSING

The universal crossed molecular beam setup and the supersonic carbon source have been described earlier in detail (Lee et al. 1969; Kaiser & Suits 1995). Briefly, the 30 Hz, 35-40 mJ per pulse, 266 nm output of a Spectra Physics GCR-270-30 Nd:YAG laser is focused on a rotating carbon rod. Ablated carbon atoms were seeded either into neon or helium carrier gas released by a Prock-Trickl pulsed valve driven with 60 Hz, 80 μs pulses and 4 atm backing pressure. A chopper wheel situated 40 mm after the laser ablation zone operates at 240 Hz and

selects a 9.0 μs section of the carbon beam. The carbon and the continuous hydrocarbon beam pass through skimmers with apertures of 1.0 mm and 0.58 mm and cross at 90° in the interaction region. Velocities range from 1100 to 3200 ms^{-1} (carbon beam) and 780 - 870 ms^{-1} (hydrocarbon beam) with speed ratios of 2.6 - 6.0 and 7.0 - 9.3, respectively. Reactively scattered products were monitored in the collision plane using a triply differentially pumped quadrupole mass spectrometer with a Brink-type electron-impact ionizer in the time-of-flight (TOF) mode, i.e. recording the time-dependent intensity of ions at one m/e-ratio at different laboratory scattering angles. Channel widths were chosen between 7.5 and 10 μs, and counting times ranged from 0.5 - 6 h averaged over several angular scans. The velocity of the supersonic carbon beam was monitored frequently and minor velocity drifts were corrected by adjusting the laser pulse delay. A reference angle is chosen at each experiment to normalize fluctuating carbon beam intensities and mass dial settings at the quadrupole controller.

Information on the reaction dynamics is gained by fitting the TOF spectra and the product angular distribution LAB in the laboratory reference frame using a forward-convolution routine (Vernon 1981; Weiss 1986). This iterative approach initially guesses the angular flux distribution $T(\theta)$ and the translational energy flux distribution $P(E_T)$ in the center-of-mass system (CM) which are assumed to be independent of each other. Laboratory TOF spectra and the laboratory angular

distribution were calculated from the $T(\theta)$ and $P(E_T)$ averaged over a grid of Newton diagrams and the apparatus functions. Best TOF and laboratory angular distributions were achieved by iteratively refining adjustable $T(\theta)$ and $P(E_T)$ parameters. Finally, a center-of-mass flux contour map $I(\theta, E_T) \sim T(\theta) * P(E_T)$, which contains all the dynamical information of the reactive scattering process, is computed.

3. RESULTS

3.1. REACTIVE SCATTERING SIGNAL

The carbon-hydrogen exchange channels (1) - (4) dominates the product distributions, and reactive scattering signal was only observed at m/e = 37, 51, 39, and 53, i.e. C_3H (reaction 1), C_4H_3 (reaction 2), C_3H_3 (reaction 3), and C_4H_5 (reaction 4). The observation of these reaction channels under single collision conditions alone underlines the potential importance of this reaction class to build up carbon-bearing molecules in interstellar environments. TOF spectra recorded at lower m/e values 36 (reaction 1), 48 - 50 (reaction 2), 36 - 38 (reaction 3), and 48 - 52 (reaction 4) show identical patterns indicating the signal originates in cracking of the parent in the detector. In addition, no radiative associations to C_3H_2, C_4H_4, C_3H_4, and C_4H_6 or higher masses were observed.

3.2. LABORATORY ANGULAR DISTRIBUTIONS

Fig. 2 displays the laboratory angular distributions (LAB) of C_3H (1), C_4H_3 (2), C_3H_3 (3), and C_4H_5 (4) at selected collision energies E_{coll} of 8.8 (1), 20.4 (2), 17.1 (3), and 23.3 $kJmol^{-1}$ (4) together with the most probable Newton diagrams and flux contour maps. The LAB distributions of reactions (2) - (4) are very broad, and products are spread at least over a range of 60^0, whereas reactive scattering signal of (1) is confined to ca. 40^0 in the scattering plane. Comparison of these scattering ranges with limit circles of different structural isomers confines energetically accessible C_3H_3 products to the propargyl, cyclopropen-1-yl or propyn-1-yl isomer. The explicit limitation to distinct C_3H, C_4H_3, and C_4H_5 isomers solely based on limit circles is not possible, since individual circles are blurred out due to the velocity spread of the carbon beam (§ 2). Further, the mass ratio of the hydrocarbon radical and H products of 39 to 53 as well as the large width of the laboratory angular distribution in (2) - (4) suggest that the translational energy distribution $P(E_T)$ peaks well away from zero and that the averaged translational energy release $\langle E_T \rangle$ is large.

3.3. CENTER-OF-MASS TRANSLATIONAL ENERGY DISTRIBUTIONS, $P(E_T)$

Best fits of TOF spectra and LAB distributions were achieved with $P(E_T)$s extending to a maximum translational energy, i.e. the sum of the reaction exothermicity and relative collision energy, of E_{max} = 30 - 90 $kJmol^{-1}$ (1), 230 - 255

kJmol^{-1} (2), 225 - 255 kJmol^{-1} (3), and 210 - 230 kJmol^{-1} (4). The order of magnitude of this high energy cut-off can be employed to identify the product isomer if their energetics are well separated. Within the error limits, data are consistent with the formation of n-C_4H_3 {3a}/{3b} (reaction 2; Kaiser et al. 1996a), the propargyl radical C_3H_3 {4} (reaction 3; Kaiser, Lee, & Suits 1996a), and the 1- and/or 3-methylpropargyl radical {5}/{6} (reaction 4; Kaiser et al. 1996b), Fig. 3. The linear {2} and cyclic C_3H {1} isomers cannot be separated based solely on the $P(E_T)$s since both enthalpies of formations differ only by about 7.5 kJmol^{-1} (Ochsenfeld et al. 1996).

In addition, the most probable translational energy gives the order-of-magnitude of the barrier height in the exit channel. All $P(E_T)$s of (2) - (4) show a broad plateau between 30 - 60 kJmol^{-1}. These data suggest a tight transition state and a significant geometry as well as electron density change from the decomposing collision complexes C_4H_4 (2), C_3H_4 (3), and C_4H_6 (4). The existence of a non-negligible exit barrier is verified by the large fraction of energy released into translational motion of the reactants to ca. 25 % (2), 35 % (3), and about 30 % (4). Our data rather suggest tight exit transition states. $P(E_T)$s of (1), however, peak at only 6 - 8 kJmol^{-1} and indicate a minor electron density change to the products (Kaiser, Lee, & Suits 1995).

3.4. CENTER-OF-MASS ANGULAR DISTRIBUTIONS, T(θ)

3.4.1. GENERAL FEATURES

The weak polarization of all center-of-mass angular distributions can be understood in terms of total angular momentum conservation and angular momentum disposal (Miller, Safron, & Herschbach 1967; Miller 1969). Based on the classical vector model, the total angular momentum **J** is given by

(5) $$\mathbf{J} = \mathbf{L} + \mathbf{j} = \mathbf{L'} + \mathbf{j'}$$

with the initial and final orbital angular momentum **L** and **L'** perpendicular to the initial and final relative velocity vectors **v** and **v'**, and **j** and **j'** the rotational angular momenta of reactants and products. Since the reactions of $C(^3P_j)$ with unsaturated hydrocarbons proceed within orbiting limits (Haider & Husain 1993; Husain 1993; Clary et al. 1994) and our relative cross sections rise as the collision energy decreases (Kaiser et al. 1996a,b), we estimate upper limits of **L** to $90\hbar$ at the lowest (8.8 $kJmol^{-1}$) and $140\hbar$ at highest (45 $kJmol^{-1}$) collision energies (Levine & Bernstein 1987; Clary et al. 1994; Kaiser, Lee, & Suits 1996a). Comparing the magnitude of **L** and **j** at typical rotational temperatures of the hydrocarbon molecules of about 20 - 40 K (j = 2 - 4), we find **L** >> **j**, and (5) reduces to

(6) $$\mathbf{L} \approx \mathbf{J} = \mathbf{L'} + \mathbf{j'}.$$

To account for the weak T(θ) polarizations, **L** and **L'** must be uncoupled and **j'** >> **L'**, hence

(7) $$\mathbf{L} \approx \mathbf{J} \approx \mathbf{j'}.$$

This weak **L**-**L'** correlation is a direct result of the inability of the light hydrogen atom to carry significant orbital angular momentum as well as of large impact parameters contributing to the initially formed triplet collision complex via capture.

3.4.2. REACTION C + C_2H_2 (1)

As the collision energy increases from 8.8 to 28.7 $kJmol^{-1}$ for this reaction, the center-of-mass angular distribution exhibits a less pronounced forward-peaking, and the intensity ratios at the poles diminish from $I(0^0)/I(180^0)$ = 2.6 to 1.2. Raising the collision energy by additional 16.3 $kJmol^{-1}$ to 45 $kJmol^{-1}$ yields an isotropic T(θ) which is symmetric around $\pi/2$. This behavior suggests two microchannels, an isotropic channel at 8.8, 28.7, and 45.0 $kJmol^{-1}$ (# 1) and a second, forward-peaked contribution at 8.8 and 28.7 $kJmol^{-1}$ quenched with rising collision energy (# 2). The asymmetric T(θ) of microchannel 2 implies a C_3H_2 complex with a lifetime shorter than its rotational period fragmenting via an asymmetric exit transition state. A symmetric transition state would result in a

center-of-mass angular distribution symmetric around $\pi/2$ despite a complex lifetime shorter than its rotational period, since the hydrogen atom can depart with equal probability in θ and π-θ. Microchannel 1 involves either a symmetric exit transition state or passes through a deep potential well with a lifetime of the fragmenting complex longer than its rotational period.

3.4.3. REACTIONS C + CH_3CCH (2) AND C + C_3H_6 (4)

At lower collision energies, $T(\theta)$s of (2) and (4) are isotropic and symmetric around $\pi/2$ implying that either the fragmenting C_4H_4/C_4H_6 complexes hold lifetimes longer than their rotational periods or that their exit transition states are symmetric. With increasing collision energy, the forward peaking $T(\theta)$ of (2) corresponds to a reduced lifetime of the decomposing C_4H_4 complex and suggests an osculating complex model: a complex formation takes place, but the well depth along the reaction coordinate is too shallow to allow multiple rotations, and the complex fragments before one full rotation elapses. Based on the intensity ratio of $T(\theta)$ at $\theta = 0°$ and 180° of 1.7± 0.1, the identification of the decomposing complex enables us to use its rotational period as a molecular clock and estimate its lifetime (§ 4). The forward peaking implies an opposite location of the incorporated carbon and leaving hydrogen atom in the fragmenting complex.

3.4.4. REACTION C + C_2H_4 (3)

Both T(θ)s show a decreasing fraction of forward-peaking reactive scattering signal with rising collision energy from 17.1 to 38.3 $kJmol^{-1}$. These data indicate the reaction proceeds via two microchannels, the first one isotropic, and the second channel forward scattered with respect to the carbon beam. Further, the exit transition state of this micromechanism has to be asymmetric. Again, the incorporated carbon and the leaving hydrogen atom must be located on opposite sites of the rotation axis.

3.5. ROTATIONAL EXCITATION OF HYDROCARBON RADICALS

The rotational constants classify the l-C_3H_3, n-C_4H_3, and C_4H_5 radicals as highly prolate asymmetric tops with asymmetry parameters κ between κ = -0.996 and -0.999 (Kaiser et al.1996a,b; Kaiser, Lee, & Suits 1996a,b). Therefore, the rotational energy levels follow in good approximation those of a rigid, symmetric top:

(8) $$E = hc\left[BJ(J+1) + (A-B)\,K^2\right].$$

J denotes the rotational quantum number, K the component of the rotational angular momentum about the principal axis, with K = 0 for no rotation about the figure axis, but perpendicular to it, and K ≈ J for a fast rotation about the principal

axis, with a slow end-over-end one. Since no explicit information on the K-distribution is available, we compute the highest accessible K state, K_{max}, assuming no vibrational excitation of the products. This gives us the upper limit of the product rotational excitation and the lowest tilt angles α_{min} of the figure axis with respect to **j'** in terms of the classical vector model to

(9) $$\alpha_{min} = \arccos(K_{max}/j').$$

Plugging all values in (9) yields, even in the case of no vibrational excitation, an average tilt angle between 68 - 80° with respect to **j'**. This clearly indicates dominant end-over-end-rotations of l-C_3H_3, n-C_4H_3, as well as C_4H_5. The rotation axes of the C_3H isomers are discussed in § 4.1.

4. CHEMICAL DYNAMICS

In the following section, we outline the chemical dynamics of reactions (1)-(4). The involved PESs are discussed and trajectories conserving highest possible symmetry to excite rotational motions of the collision complex via addition are given. Insertion into carbon-hydrogen (reaction (1) - (4)) and carbon-carbon single bonds (reacion (2) and (4)) as well as intersystem crossing (ISC) to the singlet surface do not contribute to the reactive scattering signal, since the expected chemical dynamics of both processes do not correlate with the

experimentally observed center-of-mass angular and translational energy distributions (Kaiser et al.1996a,b; Kaiser, Lee, & Suits 1996a,b).

4.1. REACTION C + C_2H_2 (1)

Fig. 4 displays a schematic energy diagram of the triplet C_3H_2 PES and feasible exit channels to l/c-C_3H. As outlined in section 3.2, microchannel 1 requires a symmetric exit transition state to explain the collision energy independent shape of the center-of-mass angular distribution. A decomposition of trans propendiylidene {7} as well as cyclopropenylidene {8} to C_3H + H can be ruled out, since any rotation around the A, B, or C-axis do not interconvert both hydrogen atoms. Considering the point groups of remaining triplet C_3H_2 isomers, only C-H-bond ruptures in propendiylidene {9} rotating around its A-axis or propargylene {10} excited to B-like rotations depict symmetric transition states. If {9} formed the l-C_3H isomer, this pathway would enforce energetically inaccessible rotations around the internuclear l-C_3H axis. A decomposing propargylene complex {10}, however, gives rise to B-like rotations of l-C_3H, and contributes to the reactive scattering signal at m/e = 37. The prevailing question is the formation of {11} itself. Based on the narrow range of impact parameters, insertion of C(^3P_j) into the acetylenic C-H-bond can be excluded (Kaiser, Lee, & Suits 1996a), and a [2,3]-H shift in {7} represents the only alternative pathway.

The primary triplet propendiylidene complexe {7} is formed via addition of $C(^3P_j)$ to one carbon atom in the acetylene molecule, c.f. 4.2. - Microchannel 2 follows direct chemical dynamics and lead to the cyclic C_3H isomer (Kaiser, Lee, & Suits 1996b).

4.2. REACTION C + CH_3CCH (2)

Conserving the C-C-C-C-plane as a symmetry element, the singly occupied $C(^3P_j)$ p_x- and p_z-orbitals add to the π_x- and π_z-orbitals of the β-C-atom under C_s symmetry to triplet cis or trans 1-methylpropendiylidene {11}/{12} (Kaiser et al. 1996a). This pathway supports a maximum orbital overlap to the newly formed C-C-σ- and C-C-π-bonds through interaction of p_x- with π_x- as well as p_z- with π_z-orbital and does not force a C-atom trajectory perpendicular to the methylacetylene molecular axis. Approach geometries with oblique angles between the carbon atom velocity vector and the C-C-C-axis are supported likewise and make larger impact parameters available for reaction. Since $\mathbf{L} \approx \mathbf{j'}$, all carbon atoms rotate in a plane approximately perpendicular to **L** around the C-axis of 1-methylpropendiylidene. The consecutive hydrogen shift to triplet 1-methylpropargylene {13} conserves the C-rotation axis. The enclosed carbon atom and the departing hydrogen of the methyl group are located on opposite sites of the rotation axis, and fulfil the requirement to explain the forward-peaked $T(\theta)$

at higher collision energy. This almost in-plane rotation yields extremely low K values as well as a minor **J** component about the figure axis of 1-methylpropargylene {13} and can be correlated to low K states populated in n-C_4H_3 after fragmentation of {13} via H-emission within 1-2 ps.

4.3. REACTION C + C_2H_4 (3)

Maintaining the C-C-C-plane as a plane of symmetry, C(^3P_j) adds perpendicular to the C_2H_4 molecular plane on the triplet surface conserving C_s symmetry (Kaiser, Lee, & Suits 1996b). This approach supports on-axis as well as off-axis trajectories of the atomic carbon p-orbital toward a C-p-orbital of the ethylene molecule. Since **L** and **L'** are weakly correlated, the three heavy atoms rotate in a plane roughly perpendicular to **L** around the C-axis of the prolate cyclopropenyl adduct {14}. The successive conrotatory ring opening to triplet allene {16} conserves C_s symmetry and converts the previously out-of-plane H-atoms into the symmetry plane. Again, the dominating in-plane rotation around the C-axis yields extremely low K values and can be related to preferentially low K states populated in the propargyl radical. The forward scattered microchannel 2 arises from C-like rotations of the triplet allene complex.

4.4. REACTION C + C_3H_6 (4)

Hitherto, we have not investigated reaction (4) at higher collision energies and cannot apply the $T(\theta)$ to identify the location of the incorporated carbon atom with respect to the leaving hydrogen, the rotation axis, and ideal approach geometries. The explicit identification of 1-and/or 2-methylpropargyl based on the translational energy distribution, however, implies that the approaching carbon atom adds to the propylene carbon-carbon double bond forming 1-methylcyclo-propylidene {16}(Kaiser, Lee, & Suits 1996b). The consecutive conrotatory ring opening leads to triplet trans/cis 1-methylallene {17/{18. Most likely, the low K values of the methylpropargyl arise from an in-plane rotation of {17/{18 around its C-axis. The H1 loss yields the 1-methylpropargyl radical, whereas C3-H2/C3-H3 bond rupture forms 3-methylpropargyl. Both isomers differ by only 3 $kJmol^{-1}$ and cannot be distinguished based on our present experimental data.

5. ASTROPHYSICAL IMPLICATIONS

The crossed molecular beam technique has been proven a powerful tool to investigate neutral - neutral reactions of potential importance to interstellar chemistry. Besides identification of distinct product isomers, information on chemical dynamics, involved collision complexes, their lifetimes, and intermolecular rearrangements are also supplied. Even in molecular clouds, the

intermediate C_3H_2, C_3H_4, C_4H_4, and C_4H_6 collision complexes cannot be isolated, but dense planetary atmospheres or cometary comae supply stabilizations or successive reactions via a third body encounter. Most important, the explicit identification of the carbon-hydrogen exchange channel to l/c-C_3H, n-C_4H_3, propargyl, and methylpropargyl radicals under single collision conditions represents an alternative pathway to competing ion-molecule reactions. The ionization of neutral carbon atoms (10), for example, initiates a four step mechanism to C_3H via ion - molecule reaction of singly ionized carbon with acetylene (11) followed by radiative association (12) and dissociative recombination (13). This sequence is in contrast to a single C - C_2H_2 encounter forming C_3H (1):

(10) $$C(^3P_j) \rightarrow e^- + C^+$$

(11) $$C_2H_2 + C^+ \rightarrow \text{l/c-}C_3H^+ + H$$

(12) $$\text{l/c-}C_3H^+ + H_2 \rightarrow \text{l/c-}C_3H_3^+ + h\nu$$

$$\rightarrow \text{l/c-}C_3H_2^+ + H$$

(13a) $$\text{l/c-}C_3H_3^+ + e \rightarrow \text{l/c-}C_3H_2 + H$$

$$\rightarrow \text{l/c-}C_3H + 2\,H\,(H_2)$$

(13b) $$\text{l/c-}C_3H_2^+ + e \rightarrow \text{l/c-}C_3H + H.$$

The actual contribution of carbon - unsaturated hydrocarbon reactions to complex species in interstellar environments depends strongly on the imposed

synthetic chemical reaction network and minor entrance barriers to the PES. Based on the molecular cloud model of Millar et al. (1987) and Betten et al. (1995), reactions of N as well as O atoms are thought to be rate limiting and destroy produced complex molecules. Very recent rate calculations of (14), however,

(14) $C_3(^1\Sigma_g^+) + O(^3P_j) \rightarrow CO(^1\Sigma^+) + C_2(^3\Pi)$

do not support this conclusion - at least for the C_3 carbon cluster - since an entrance barrier of 7.5 kJmol^{-1} inhibits this reaction in warm as well as cold intestellar clouds (Woon & Herbst 1996). Unlike this scenario, inclusion of C atom reactions in a model of the circumstellar envelope surrounding the carbon star IRC+10216 does not lead to a destruction of complex, carbon bearing species since the ratio of atomic carbon to oxygen is greater than unity. Further, lowest investigated collision energies of 8.8 kJmol^{-1} in our experiments are equivalent to about 900 K versus a maximum translational temperature of ca. 100 K in molecular clouds, but up to 4500 K in outflow of carbon stars. Although our data depict rising reaction cross sections as the collision energy falls (Kaiser et al. a, b 1996; Kaiser, Lee, & Suits 1996), extrapolation to interstellar temperatures as low as 10 - 100 K depends on the absence of even small barriers. A strong interplay of crossed beam experiments and low temperature kinetic studies is desirable.

Our findings should encourage an actual search for the hitherto unobserved radicals l-C_3H_3, n-C_4H_3, and l-C_4H_5. In particular, methylacetylene has been

widely observed toward, e.g., the orion ridge, Sagattarius B2, and TMC-1 (Irvine et al. 1987). These clouds serves as ideal targets to identify potential C_4H_3-isomers, perhaps in unidentified microwave transitions in the spectrum toward the extended ridge of OMC-1 (Sutton et al. 1995).

ACKNOWLEDGEMENTS

R.I.K. is indebted the Deutsche Forschungsgemeinschaft for a post-doctoral fellowship and the IAU for financial support to present these results on the IAU symposium 178 ''Molecules in Astrophysics: Probes and Processes" in Leiden, The Netherlands. This work was further supported by the Director, Office of Energy Research, Office of Basic Energy Sciences, Chemical Sciences Division of the U.S. Department of Energy under Contract No. DE-AC03-76SF00098.

REFERENCES

Bettens, R.P.A. & Herbst, E. 1995, Int. J. Mass Spectr. Ion. Proc., 149/150, 321.

Bettens, R.P.A., Lee, H.H., & Herbst, E. 1995, Ap.J., 443, 664.

Black, J.H. & Dalgarno, A 1973, Astrophys. Let., 15, 79.

Canosa, A., Sims, I.R., Travers, D., Smith, I.W.M., & Rowe, B.R. 1996, to be submitted to AA.

Clary, D.C., Haider, N., Husain, D., & Kabir, M. 1994, Ap.J., 422, 416.

Clary, D.C., Stoecklin, T.S., & Wickham, A.G. 1993, J. Chem. Soc. Far. Trans. 89, 2185.

Cooksy, A.L.. 1995, J. Am. Chem. Soc., 117, 1098.

Cowley, C.R. 1995, An Introduction to Cosmochemistry (Cambridge: Cambridge University Press).

Gerlich, D. & Horning, S. 1992, Chem. Rev., 92, 1509.

Graff, M.M. 1989, Ap.J., 339, 239.

Haider, N. & Husain, D. 1993, J. Photochem. Photobiolo., A70, 119.

Herbst, E. & Delos, J. 1976, Chem. Phys. let., 42, 54.

Herbst, E. & Klemperer, W. 1973, Ap.J., 185, 505.

Herbst, E. & Leung, C.M. 1990, Ap.J. 233, 170.

Herbst, E., Adams, N. G., & Smith, D. 1984, Ap.J. 285, 618.

Herbst, E., Lee, H.H., Howe, D.A., & Millar, T.J. 1994, MNRAS, 268, 335.

Husain, D. 1993, J. Chem. Soc. Farad. Trans., 89, 2164.

Irvine, W. M., University of Massacusetts, presented on COSPAR, Washington D.C. (1992).

Kaiser, R. I., Lee, Y. T., & Suits, A G. 1995, J. Chem. Phys., 103, 10395.

Kaiser, R. I., Lee, Y. T., & Suits, A. G. 1996a, J. Chem. Phys., to be submitted.

Kaiser, R. I., Lee, Y. T., & Suits, A. G. 1996b, J. Chem. Phys., in press.

Kaiser, R. I., Stranges, D., Lee, Y. T., & Suits, A. G. 1996a, J. Chem. Phys., in press.

Kaiser, R. I., Stranges, D., Lee, Y. T., & Suits, A. G. 1996b, J. Chem. Phys., submitted.

Kaiser, R.I. & Suits, A.G. 1995, Rev. Sci. Instr. 66, 5405.

Kasai, P.H. 1972, J. Am. Chem. Soc., 94, 5950.

Kasai, P.H., Skattebol, L., &Whipple, E.B. 1986, J. Am. Chem. Soc., 90, 4509

Lee, Y. T. 1988, in Atomic and Molecular Beam Methods, Volume 1, ed. G. Scoles (Oxford: Oxford University Press), 553.

Lee, Y. T., McDonald, J. D., LeBreton, P. R., & Herschbach, D. R. 1969, Rev. Sci. Instr., 40, 1402.

Levine, R. D., Bernstein, R. B. 1987, Molecular Reaction Dynamics and Chemical Reactivity (Oxford: Oxford University Press).

Liao, Q. & Herbst, .E 1995, Ap.J., 444, 694.

Millar, T.J. & Herbst, E. 1994, AA, 288, 561.

Millar, T.J., Leung, C.N., & Herbst, E. 1987, AA, 183, 109.

Miller, W.B. 1969, Ph.D. thesis (Harvard University: Cambridge).

Miller, W.B., Safron, S.A., & Herschbach, D.R. 1967, Discuss. Faraday. Society, 44, 108.

Ochsenfeld, C., Kaiser, R.I., Suits, A.G., & Head-Gordon, M. 1996, J. Chem. Phys., to be submitted.

Scheffler, H. & Elsässer, H. 1988, Physics of the Galaxy and Interstellar Matter (Berlin: Springer).

Sims, I.R., Queffelec, J., Defrance, A., Rebrion-Rowe, C., Travers, D., Bocherel, P., Rowe, B.R., & Smith, I.W.M. 1994a, J. Chem. Phys., 100, 4229.

Sims, I.R., Queffelec, J., Defrance, A., Rebrion-Rowe, C., Travers, D., Rowe, B.R., & Smith, I.W.M. 1992, J.Chem.Phys., 97, 8798.

Sims, I.R., Queffelec, J., Travers, D., Bocherel, P., Rowe, B.R., Herbert, L.B., Karthauser, J.& Smith, I.W.M. 1993, Chem. Phys. Let., 211, 461.

Sims, I.R., Smith, I.W.M., Bocherel, P., Defrance, A., Travers, D., Rowe, B.R., 1994b, J. Chem. Soc. Faraday Trans., 90, 1473.

Smith, D. 1992, Chem. Rev., 92, 1580.

Sternberg, A. & Dalgarno, A. 1995, Ap.J. Supl. Ser., 99, 565.

Sutton, E.C., Peng, R., Danchi, W.C., Jaminet, P.A., Sandell, G., & Russel, A.P.G. 1995, Ap.J. Supl. Series, 97, 455.

Thaddeus, P., Vrtilek, J.M., & Gottlieb, C.A. 1985, Ap.J., 299, L63.

Vernon, M. 1981, LBL-Report 12422.

Weiss, M.S. 1986, Ph.D. thesis (University of California, Berkeley).

Woon, D.E. & Herbst, E. 1996, Ap.J. 465, 795.

Williams, D.A. 1979, Astrophys. Let., 10, 17.

Winnewisser, G., Herbst, E. 1987, in Topics in current Chemistry, 139 (Springer: Berlin), 121.

Yamamoto, S. & Saito, S. 1990, Ap.J. 363, L13.

Yamamoto, S., Saito, S., Ohishi, M., Suzuki, H., Ishikawa, S.I., Kaifu, H., & Murakami, A. 1987, Ap.J. 322, L55.

FIG. 1. Structure of reactive scattering partners with $C(^3P_j)$: acetylene (reaction 1), methylacetylene (reaction 2), ethylene (reaction 3), and propylene (reaction 4).

FIG. 2. Top: Laboratory angular distributions of C_3H (a), C_4H_3 (b), C_3H_3 (c), and C_4H_5 (d) at collision energies of 8.8 (a), 20.4 (b), 17.1 (c), and 23.3 $kJmol^{-1}$ (d). Open circles represent measured data within 1σ error bars, the solid lines the calculated distributions. Bottom: Most probable Newton diagrams and flux contour maps of (1) - (4) at collision energies of 8.8 (a), 20.4 (b), 17.1 (c), and 23.3 $kJmol^{-1}$ (d).

FIG. 3. Reactive scattering products of reactions (1) - (4): cyclopropynylidyne (c-C_3H{1}), propynylidyne (l-C_3H {2}), α-ethinylvinyl/butatrienyl (n-C_4H_3 {3a}/ {3b}), propargyl (l-C_3H_3 {4}), and 1-or 3-methylpropargyl (l-C_4H_5 {5}/{6}. The equilibrium geometry of a bent {3a} versus linear n-C_4H_3 {3b} has not yet been resolved (Kasai, Skattebol, & Whipple 1986; Kasai 1972; Cooksy 1995).

FIG. 4. Schematic potential energy diagram of the triplet C_3H_2 PES. Enthalpies of formation in $kJmol^{-1}$ and point groups are taken from Bofill et al. 1988, Maier et al. 1989, Lee et al. 1985, Jonas et al. 1992, Clauberg et al., Herges et al. and Hehre et al..

FIG. 5. Schematic potential energy diagram of the triplet C_4H_4 PES

FIG. 6. Schematic potential energy diagram of the triplet C_3H_3 PES Kaiser et al 1996b. Enthalpies of formation are in $kJmol^{-1}$. The equilibrium structure of a 1,3-diradicaloid {14a} versus carbene structures {14b}/{14c} of methylpropargylene have not yet been a subject of ab initio calculations.

FIG. 7. Schematic potential energy diagram of the triplet C_4H_6 PES modified from Kaiser et al. 1996a.

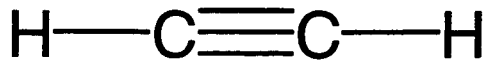

acetylene

methylacetylene

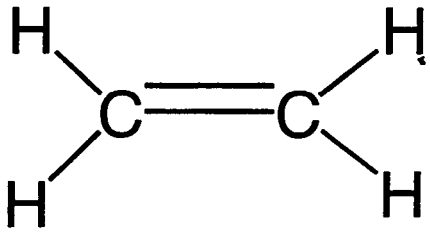

ethylene

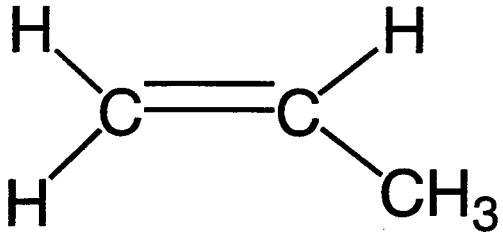

propylene

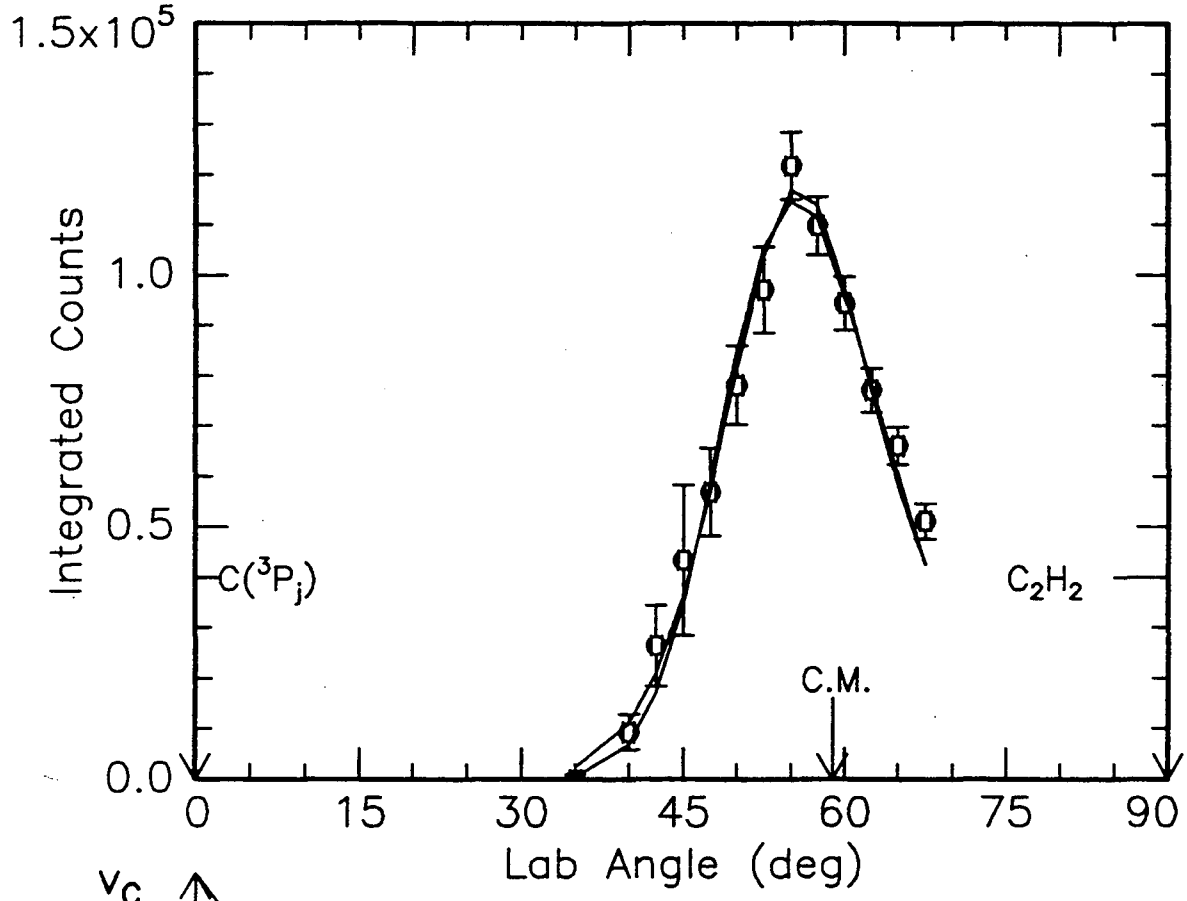
1.5x10^5
1.0
0.5
0.0
Integrated Counts
C(3Pj)
C2H2
C.M.
0
15
30
45
60
75
90
Lab Angle (deg)

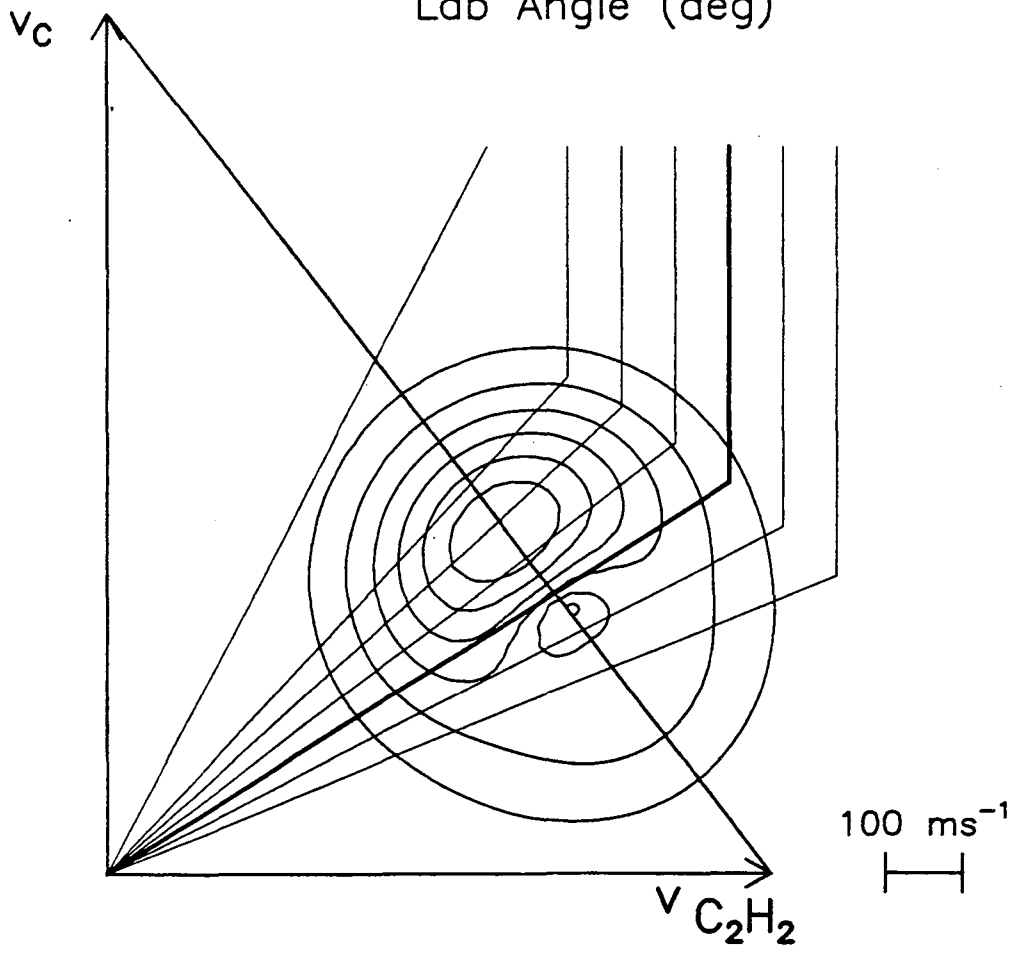
vC
100 ms-1
v C2H2

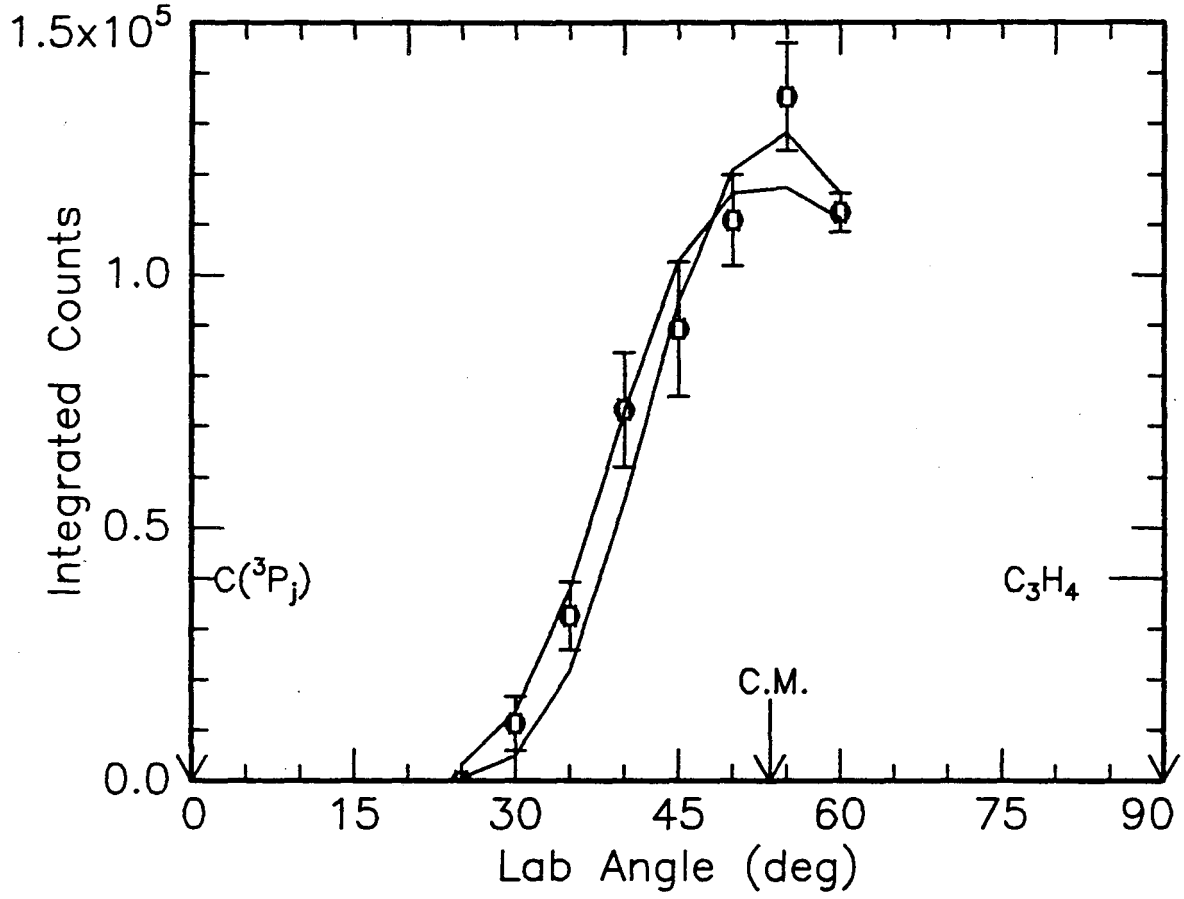
1.5x10^5
1.0
0.5
0.0
Integrated Counts
C(3Pj)
C3H4
C.M.
0
15
30
45
60
75
90
Lab Angle (deg)

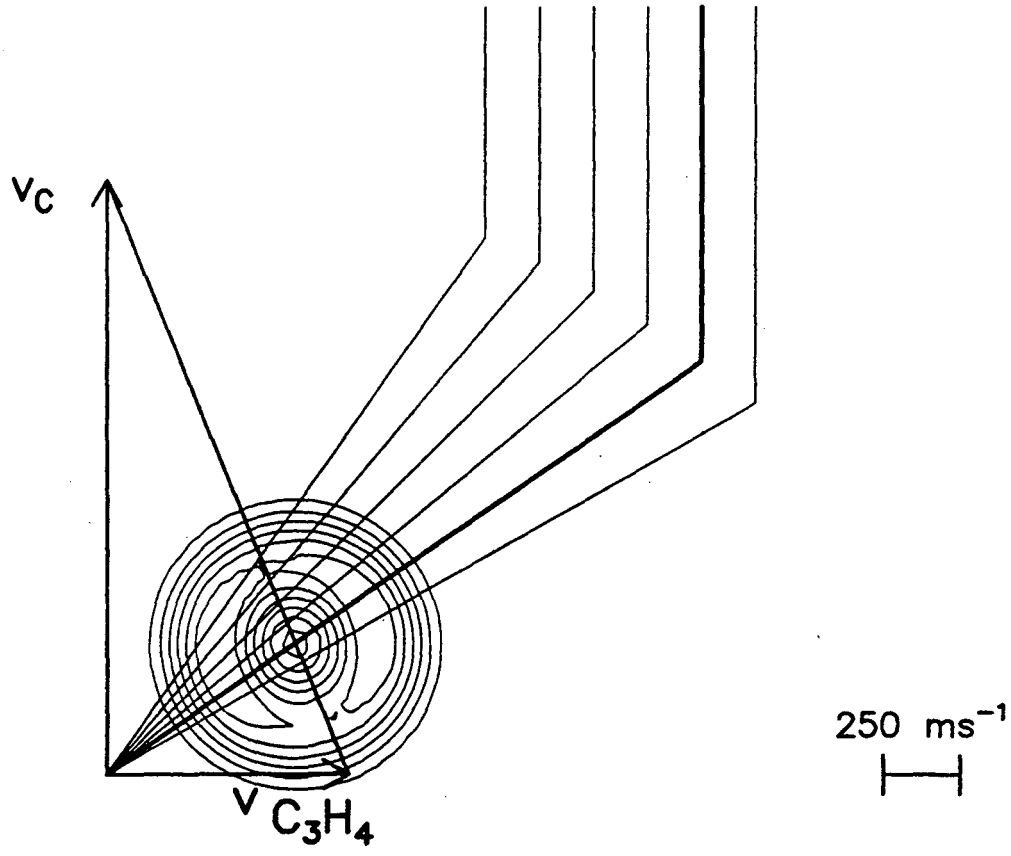
vC
v C3H4
250 ms-1

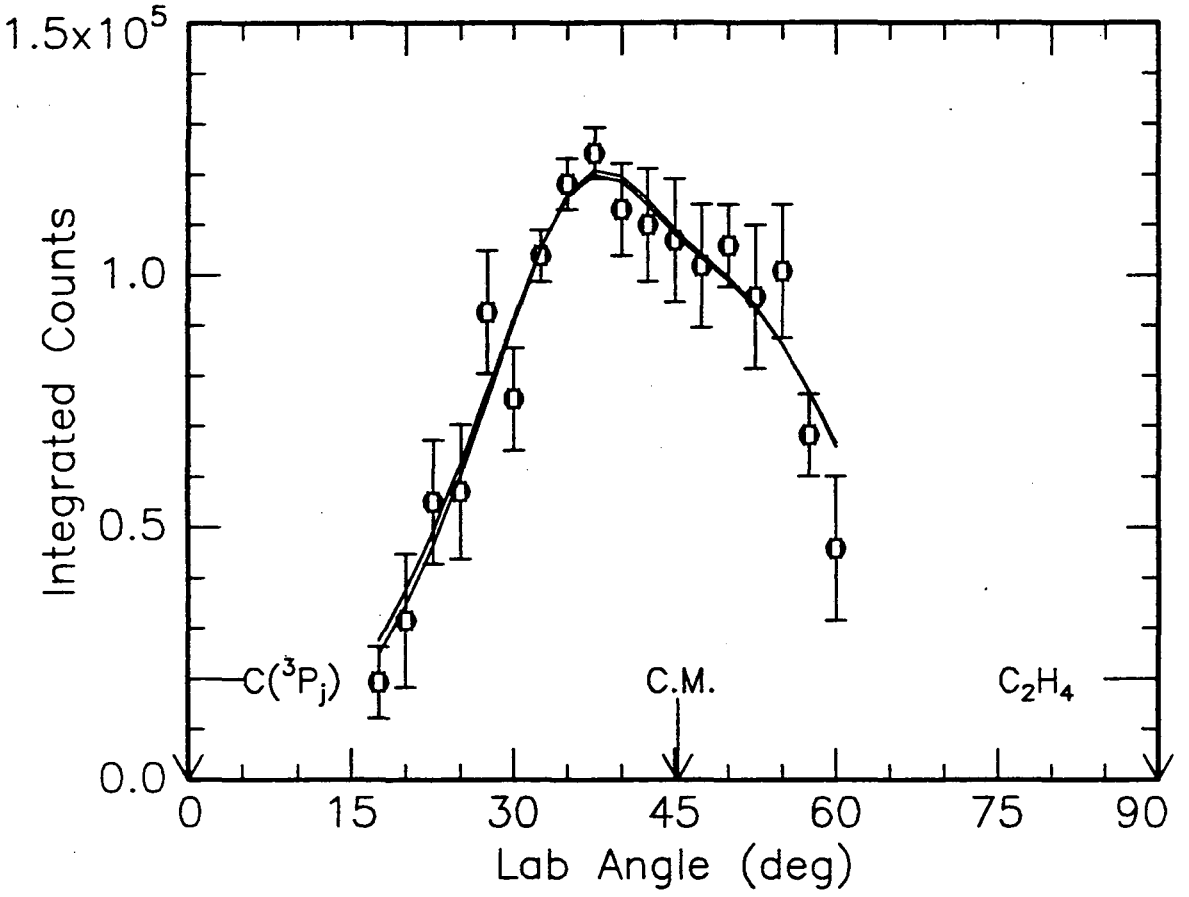
1.5x10^5
1.0
0.5
0.0
Integrated Counts
C(3Pj)
C.M.
C2H4
0
15
30
45
60
75
90
Lab Angle (deg)

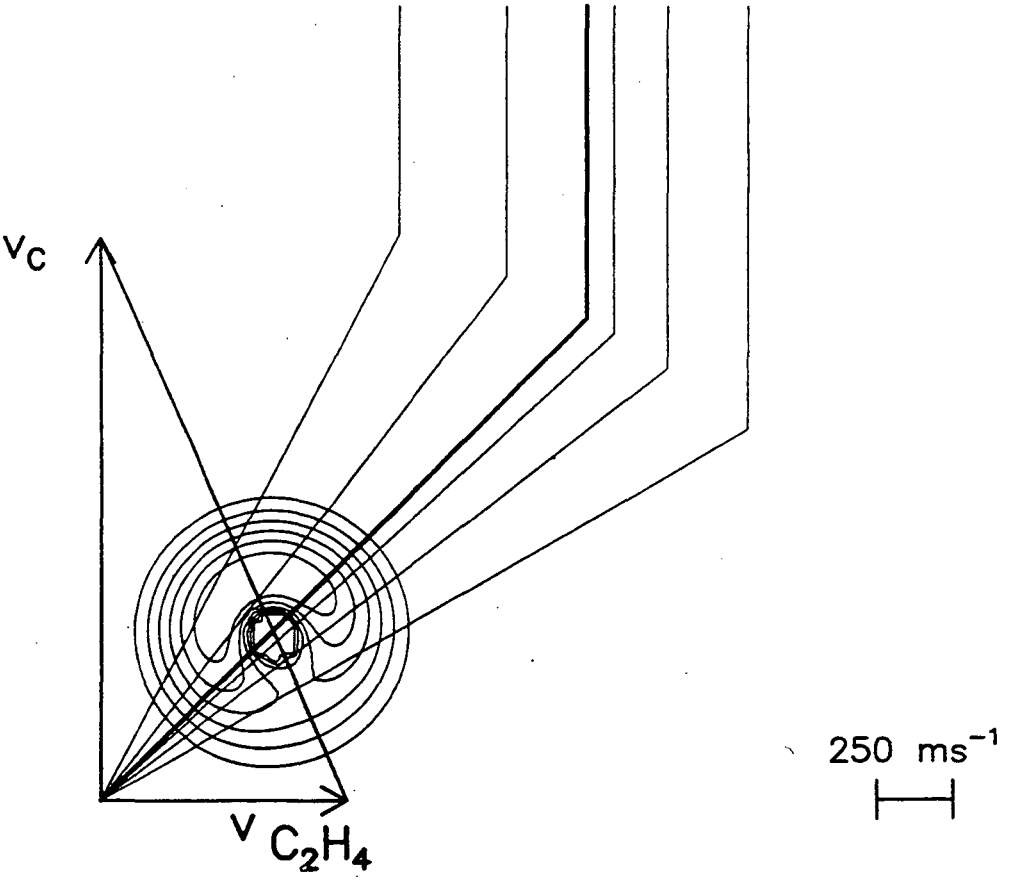
vC
v C2H4
250 ms-1

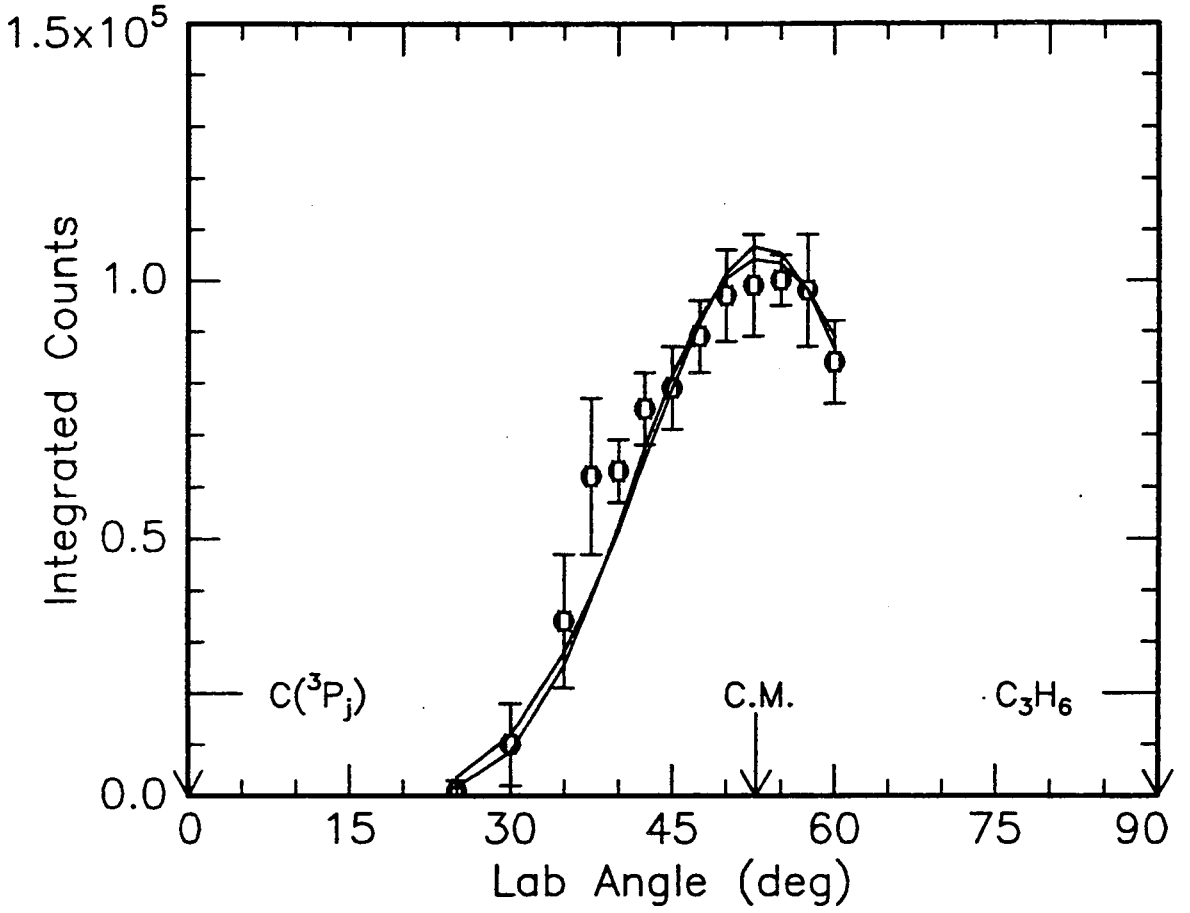
1.5x10^5
1.0
0.5
0.0
Integrated Counts
C(3Pj)
C.M.
C3H6
0
15
30
45
60
75
90
Lab Angle (deg)

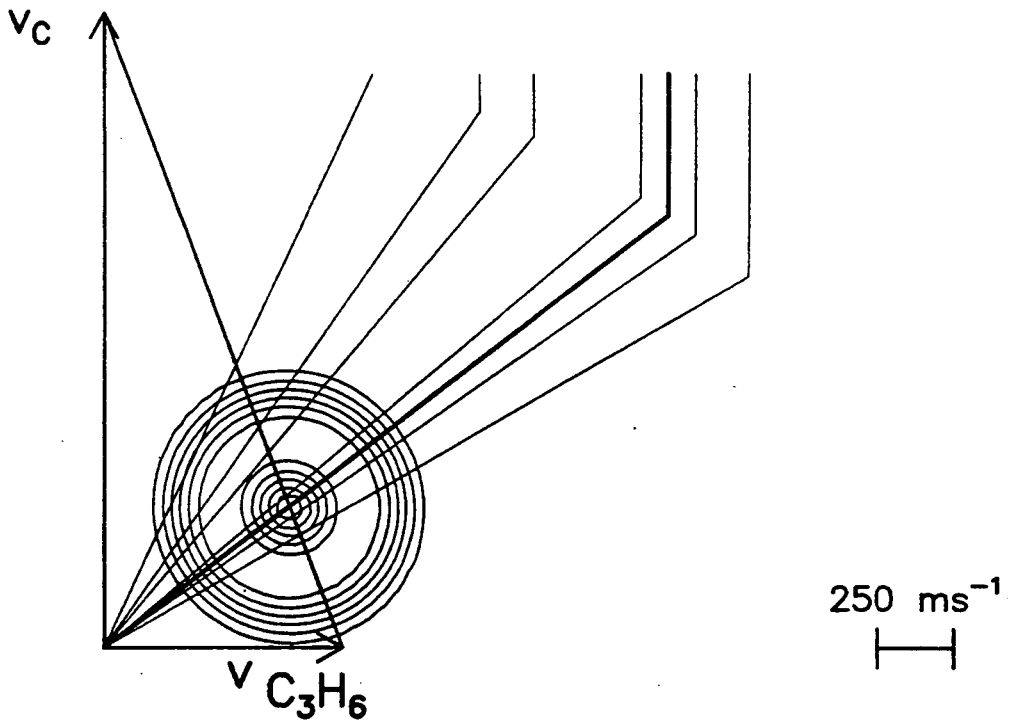
vC
v C3H6
250 ms-1

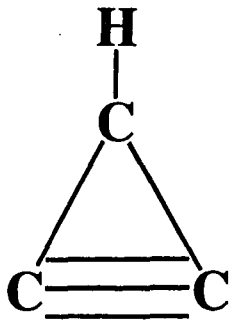

{1}

{2}

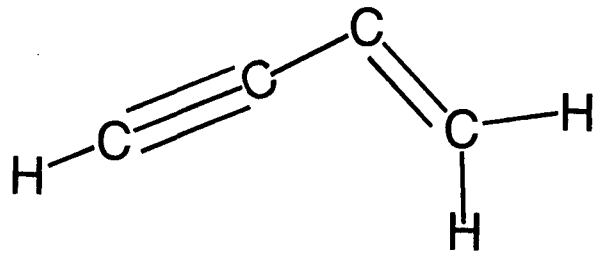

{3a}

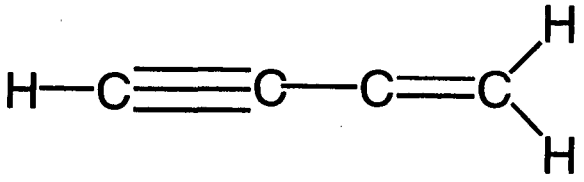

{3b}

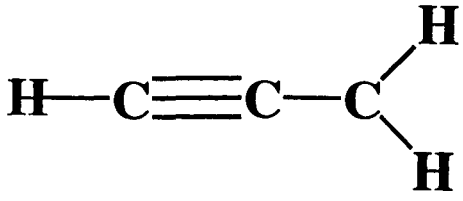

{4}

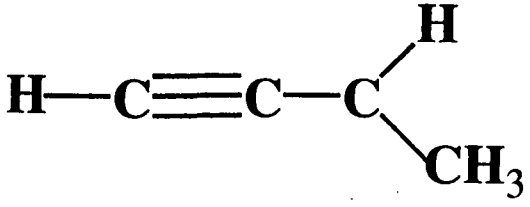

{5}

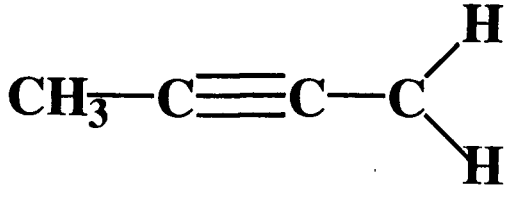

{6}

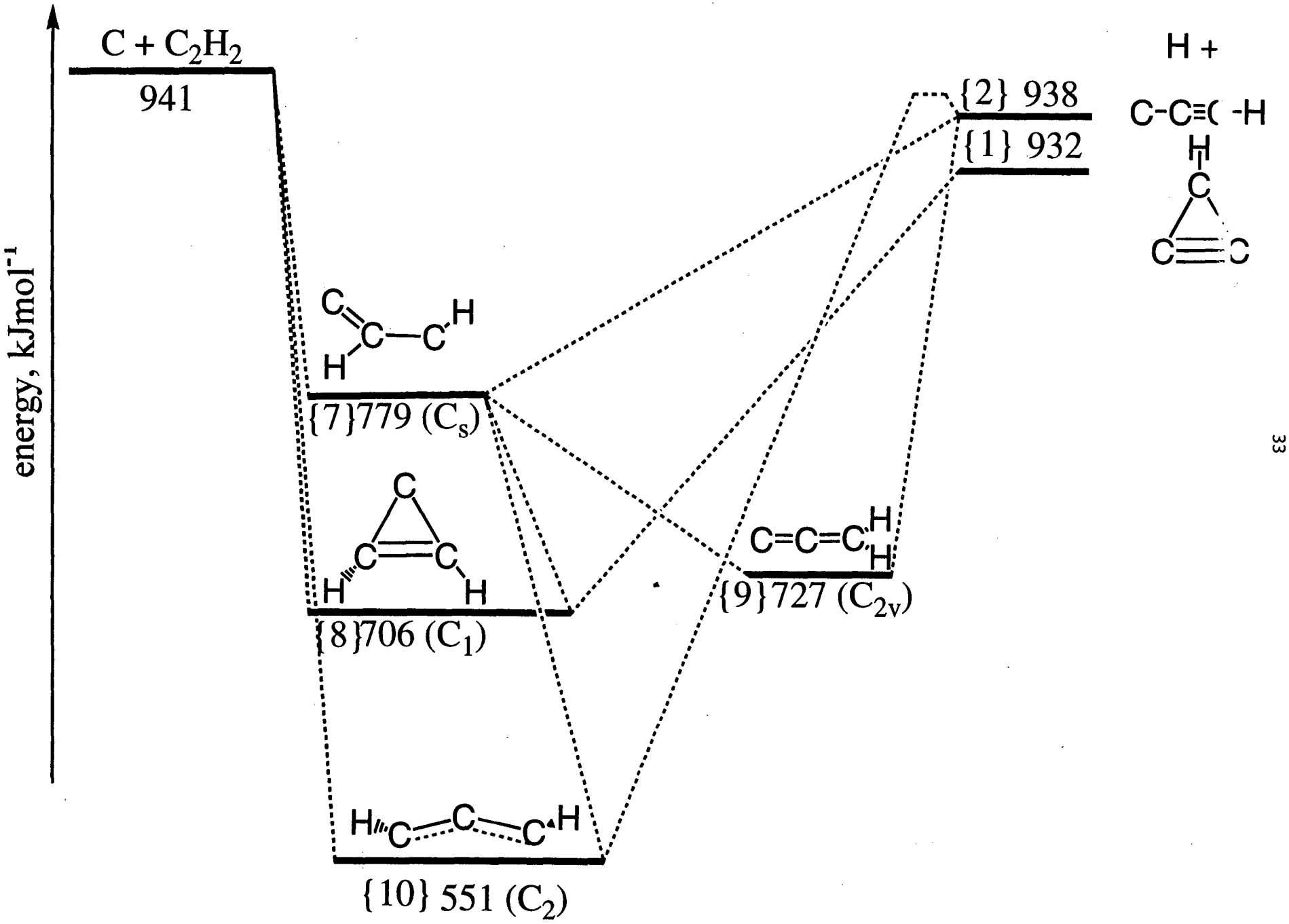
energy, kJmol-1
C + C2H2
941
{2} 938
{1} 932
H +
C-C≡C -H
H
{7}779 (Cs)
{8}706 (C1)
{9}727 (C2v)
{10} 551 (C2)

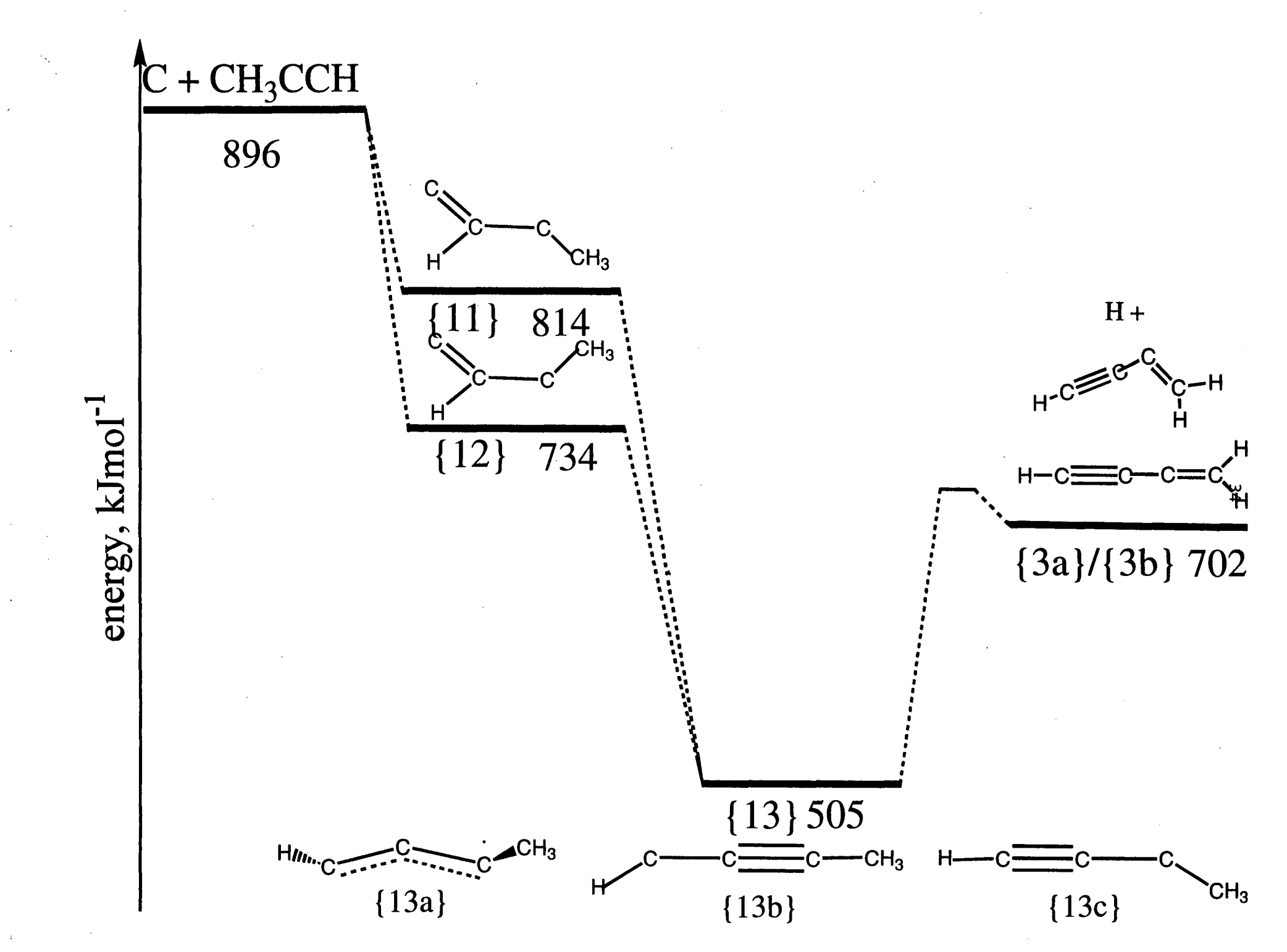
C + CH3CCH
896
{11} 814
{12} 734
H +
{3a}/{3b} 702
{13} 505
energy, kJmol-1
{13a}
{13b}
{13c}

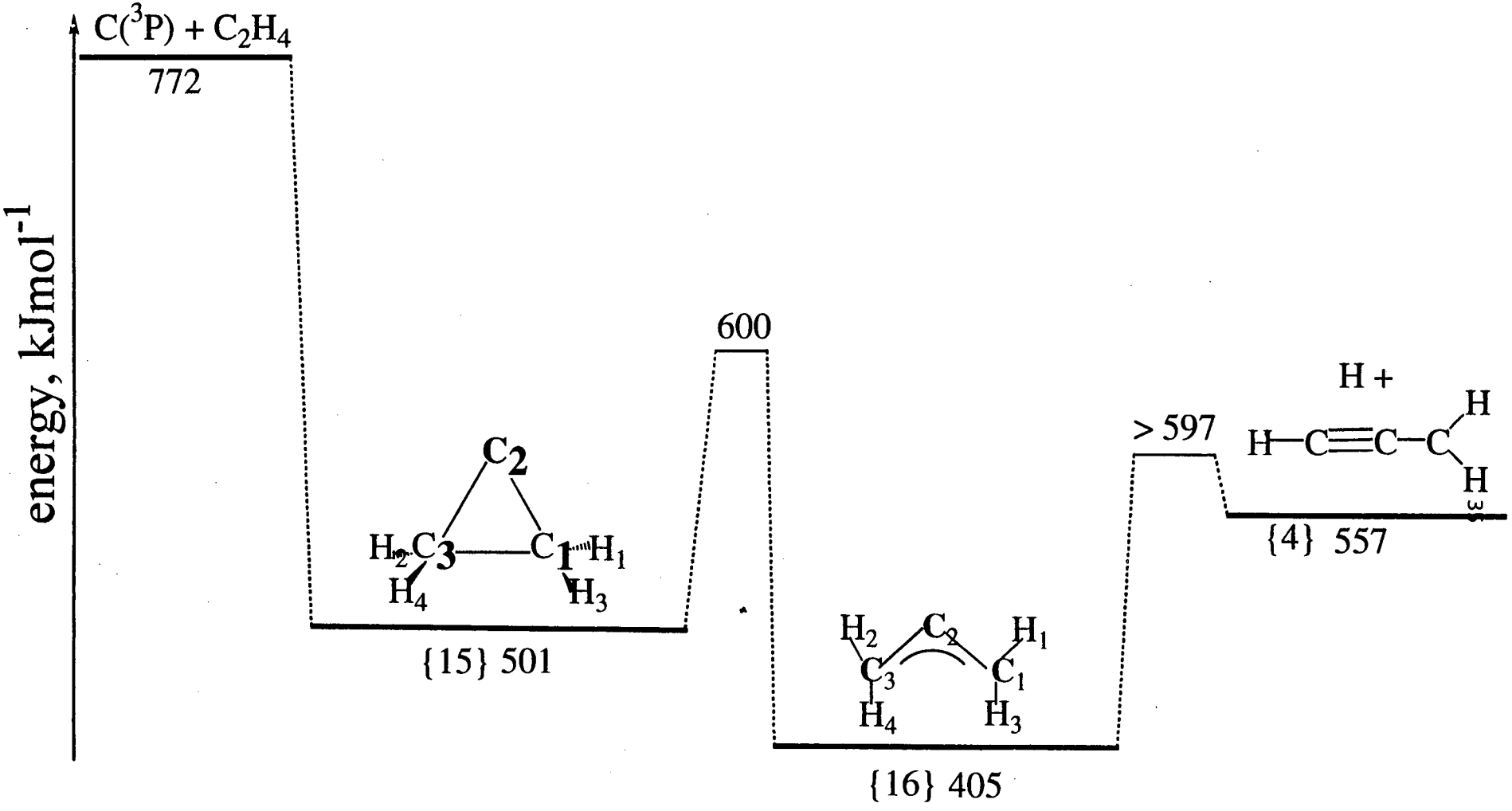
energy, kJmol-1
C(3P) + C2H4
772
{15} 501
600
{16} 405
> 597
H +
{4} 557

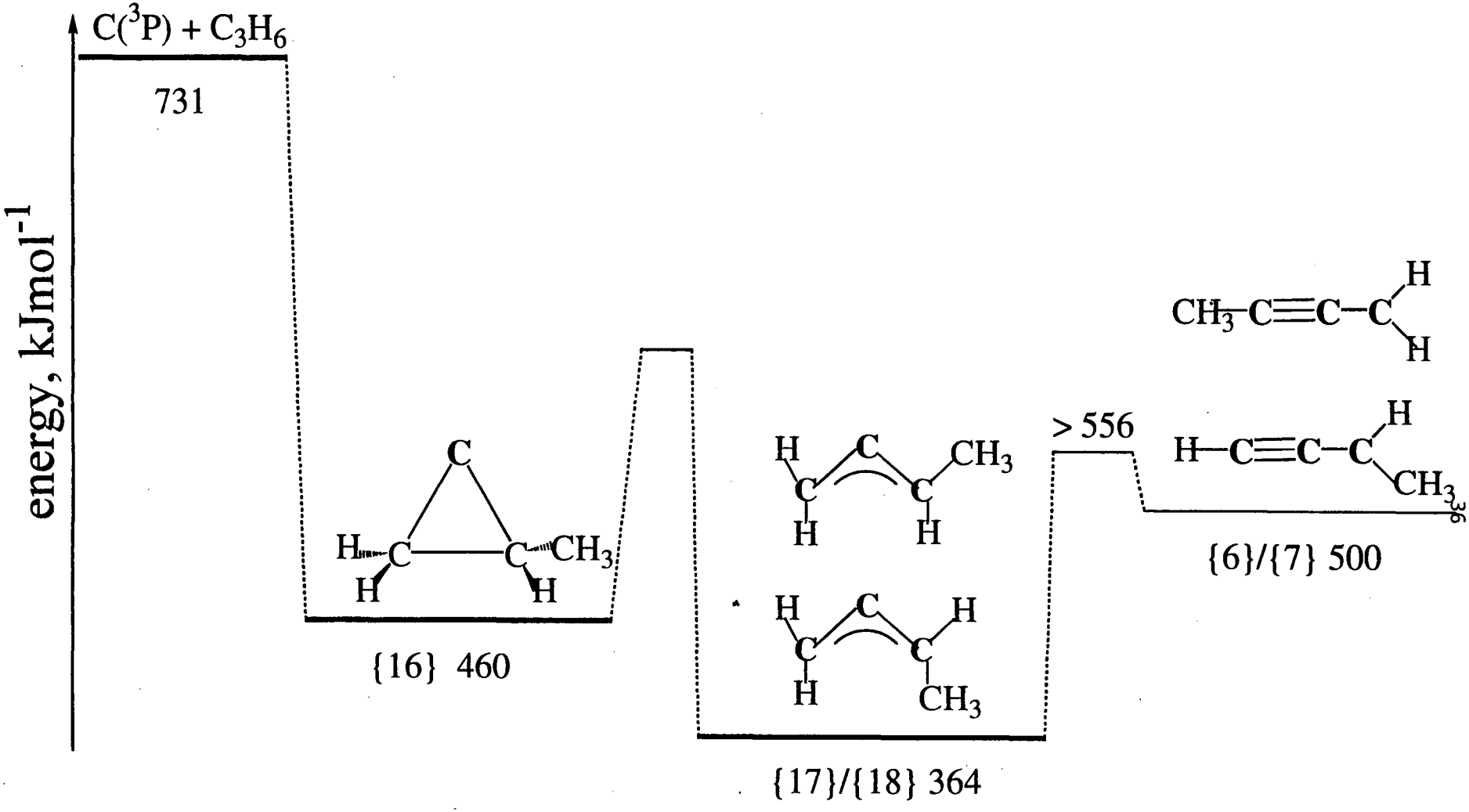
energy, kJmol-1
C(3P) + C3H6
731
{16} 460
{17}/{18} 364
> 556
{6}/{7} 500

Ernest Orlando Lawrence Berkeley National Laboratory
One Cyclotron Road | Berkeley, California 94720

Prepared for the U.S. Department of Energy under Contract No. DE-AC03-76SF00098